

# PCCP

Accepted Manuscript



This is an *Accepted Manuscript*, which has been through the Royal Society of Chemistry peer review process and has been accepted for publication.

*Accepted Manuscripts* are published online shortly after acceptance, before technical editing, formatting and proof reading. Using this free service, authors can make their results available to the community, in citable form, before we publish the edited article. We will replace this *Accepted Manuscript* with the edited and formatted *Advance Article* as soon as it is available.

You can find more information about *Accepted Manuscripts* in the [Information for Authors](#).

Please note that technical editing may introduce minor changes to the text and/or graphics, which may alter content. The journal's standard [Terms & Conditions](#) and the [Ethical guidelines](#) still apply. In no event shall the Royal Society of Chemistry be held responsible for any errors or omissions in this *Accepted Manuscript* or any consequences arising from the use of any information it contains.

# Self diffusion in nanocrystalline alloys.

Zbigniew Kaszkur,<sup>\*a</sup> Wojciech Juszczyk,<sup>a</sup> and Dariusz Łomot<sup>a</sup>

Received Xth XXXXXXXXXXXX 20XX, Accepted Xth XXXXXXXXXXXX 20XX

First published on the web Xth XXXXXXXXXXXX 200X

DOI: 10.1039/b000000x

We report operando XRD/MS experiment on nanocrystalline Pd(70%)Ag(30%) alloy supported on silica (10% wt. of metal) monitoring slow reversible Pd (in CO) and subsequently Ag (in He) surface segregation at 673K. XRD data following CO and He flow show structural changes that can be modeled and interpreted in terms of diffusion phenomena within a typical metal nanocluster. Qualitative differences of both segregation processes rate suggest different diffusion mechanism as the Pd segregation involves vacancies depletion. The experimental details suggest that this kind of experiment can provide very sensitive response to subtle changes at the surface of nanoclusters. Segregation processes can be stopped at any time by lowering temperature below 573K what allows engineering of metal surface e.g. preparing for catalytic low temperature reaction on a well defined surface.

## 1 Introduction

Our understanding of diffusion phenomena in metals date back to Kirkendall experiments<sup>1</sup> and to series of Baluffi works<sup>2-4</sup> effectively showing that the phenomenon occurs via vacancy mechanism. The latter works allowed first estimation of the vacancies density in the lattice by comparison of temperature evolution of the metal lattice constant and the sample bar length change at higher temperatures approaching melting. Such experiments are however not applicable to nanocrystalline samples and diffusion measurements in nanoparticles (NP) have to follow different scheme. The one often adopted in literature is x-ray diffraction<sup>5-7</sup>. For poly- and nanocrystals the principal diffusive transport proceeds along grain boundaries. Transport phenomena within the grains are slow at ambient temperatures but due to the diffusion path length comparable to the NPs size, may play an important role determining material properties. One phenomenon that may have large impact on the properties of the nanocrystalline material is surface segregation. For nanocrystals it has to be considered as a bulk diffusion phenomenon because atom transport involves all the crystal atoms. It is worth to notice that the transport may proceed against the concentration gradient and the phenomenon cannot be described by the Fick's laws. Instead it follows a gradient of the chemical potential. As the mean free path does not grow as a square root of time, the diffusion phenomenon has to be considered anomalous. The driving force for the transport is changing composition of the surface layer what modifies chemical potential of atoms in few subsurface layers. The atom random walk process modifies chemical potential of atoms even further transforming the process in NPs into effectively bulk phenomenon. The surface layer compo-

sition can be changing due to: (i) equilibration with the gas phase locally enriched in the element of lower heat of sublimation and lower surface tension, (ii) ion bombardment depleting the surface of the element with higher rate of sputtering, (iii) chemisorption causing one of the alloy element being kept more strongly to the surface. Then the in depth segregation process is initiated by random walk starting from the surface. Following Baluffi experiments one can expect that this diffusion process is greatly facilitated by considerable concentration of vacancies below the surface layer.

The reported work aims at shedding light onto mechanism of segregation process in PdAg nanoalloy. PdAg system is claimed to have no miscibility gap what facilitates data interpretation. On the other hand the alloy has commercial applications especially for Pd content larger than 60% when it becomes tarnish resistant. Besides hydrogen filters, low current electronic applications (contacts, capacitors) it finds a very precisely addressed use as a catalyst in many important chemical processes. It can also find use in various multifunctional devices created by a controllable growth of hybrid nanostructures as was recently shown<sup>8</sup>. We describe experiments proving that the concentration profile within the nanoalloy can be to large extent controlled and programmed. Segregation of each element can be initiated and the process monitored in time. At low temperatures the process is effectively frozen allowing e.g. catalytic low temperature reaction to be run on NPs of controlled surface composition. The presented approach follows diffusion kinetics and offers insight into mechanisms of transport in nanoalloys.

## 2 Experimental

The 10% wt. metal-loaded Pd70Ag30/SiO<sub>2</sub> (where 70 and 30 are atomic % of metals) catalyst was prepared by the incipient

<sup>a</sup> Institute of Physical Chemistry PAS, Kasprzaka 44/52, 01-224, Warszawa, Poland. Fax: 48 223433450; Tel: 48 223433284; E-mail: zbig@ichf.edu.pl

wetness coimpregnation method. The support was amorphous silica (Davison 62, 100 -120 mesh,  $300\text{m}^2/\text{g}$ ). The precursors used for preparing PdAg/SiO<sub>2</sub> were tetraamminepalladium(II) nitrate (Ventron Alfa Produkte, cat. no. 89857, Germany) and silver nitrate (analytical purity from POCh, Gliwice, Poland). The required amount of precursors were dissolved in deionized water, then contacted with the silica. During impregnation, mixing was assured by the rotary motion of a beaker containing the catalyst precursor. The resulted solid was dried at room temperature for 24 h and then further dried at 393K overnight and finally stored in a desiccator. About 50 mg samples used for measurements were spread over a thin porous sintered glass disc and mounted vertically on a stainless steel heating block of our vacuum proof XRD camera. The environmental camera of 150 ml volume was similar to the described before<sup>9</sup>, with removable cap having X-ray window secured by  $12.5\ \mu\text{m}$  self adhesive Capton foil. It was connected to the gas line via Swagelok vacuum fittings and stainless steel flexible tubings enabling XRD measurements in Bragg-Brentano geometry. The outlet gas was collected from the back side of the porous glass through the heating block assuring close contact with the sample load. Between camera and the flex-tubing an union tee fitting (Swagelok) provided splitting the stream between output and a probing capillary of a mass spectrometer (Hiden Analytical). The gas supply system and elements of the measurement control were described previously<sup>10</sup>. The gases used were helium of 99.999% purity, hydrogen (99.9995%) and CO (99.998% purity with CO<sub>2</sub> as a principal contaminant). The powder diffraction patterns were collected on D5000 powder diffractometer (Bruker AXS) equipped with LynxEye strip detector providing good resolution and quick data collection. The Cu K<sub>α</sub> radiation has been employed with X-ray tube operating at 40kV and 40mA. The XRD patterns were recorded repeatedly following the investigated process.

The whole setup was controlled by an integrated Linux client-server network architecture and the measurements could be repeatedly performed under control of measurement scripts.

The fresh sample shows multiphase diffraction pattern with maxima characteristic for fcc alloy phases but with most of Pd in form of PdO phase. Classic procedure of calcination and reduction does not provide an uniform sample. To obtain phase uniform supported alloy material we heated up the sample to 673K in carbon monoxide over 2 days. The resulting metal phase shows narrower, regular (bell shaped) peaks (fig.1). On cooling down to RT the sample was exposed to H<sub>2</sub> and undertook transition to metal hydride phase (red curve in fig.1). The new phase peaks were of practically the same width corresponding to the crystal size from the Scherrer formula of about 14 nm. This observation was proving that the metal in the final

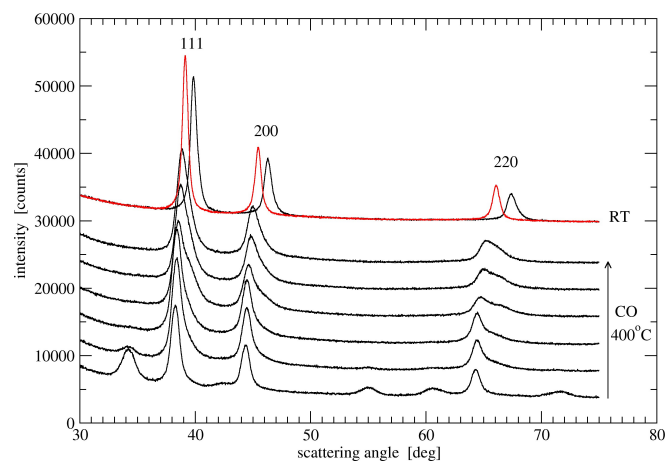


**Fig. 1** XRD pattern evolution on the sample treatment. The top curves-RT in helium (black), RT in H<sub>2</sub> (red).

sample contains alloy crystals of roughly the same elemental composition. The test bases on the literature data showing decrease in alloy peak shift on hydride formation with growing Ag contents<sup>11</sup>. It is due to the fact that silver atom added to palladium gives an electron to the unfilled part of palladium d-band, similarly like absorbed hydrogen and the electronic structure of PdAg alloy closely resembles that of PdH. PdAg alloy can thus, depending on Ag concentration, accept less hydrogen in the lattice what causes its smaller expansion<sup>11</sup>. This, together with the alloy peak position shifting to lower angles with growing Ag contents suggests that the multiphase peak should decrease its width on hydride formation. The experimental observation of diffraction maxima conserving their width may thus serve as an effective test of the sample phase uniformity. The described temperature treatment results in the material thermally equilibrated and showing no marks of a visible sintering at lower temperatures. This is why for further experiments the sample was preheated at 693K in helium.

At this stage a part of the sample has been investigated by TEM (FEI Titan CUBED 80-300) in SEM mode as well as in high resolution to compare its results with XRD data. A particle size histogram collected from measuring 450 metal particles (Fig.2) reveals average size of 6.9 nm. Various crystals contribute to the powder XRD (PXRD) pattern proportionally to their number of atoms i.e. to their volume. This is why the PXRD peak is a volume weighted average of the peaks originating from various size crystals and, similarly the peak width as well as the crystal size calculated from Scherrer formula, is a volume weighted average. Calculation of the volume weighted average of the size distribution presented in Fig.2 C gives the value of 13.1 nm. The agreement with PXRD estimation has to be considered good remembering that crystals larger than 20 nm are found on few TEM images with

large statistical error, some were excluded from the histogram but have significant impact on the average value. The qualitative analysis shows Ag located mostly in the outer shells of nanoparticles (Fig.2).

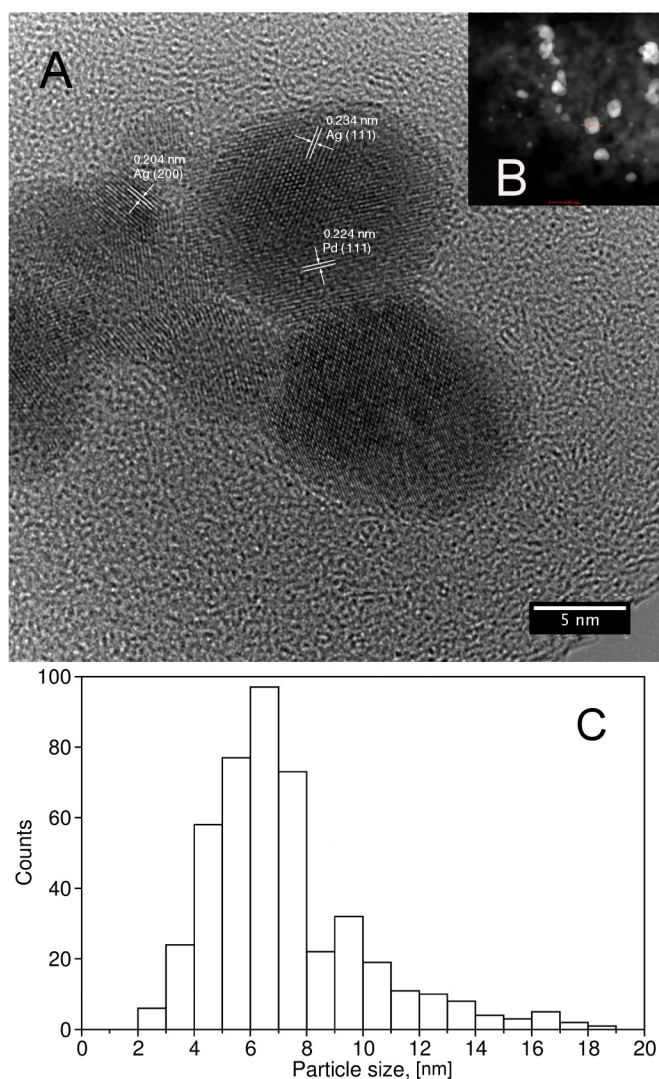


**Fig. 2** HR image of the sample preheated at 693K in He (A), the analysis of interplanar distances reveals Ag mostly in outer parts of NPs; insert shows SEM image of alloy particles distributed on the support (B); bottom - histogram of crystal size of 450 probed alloy particles (C).

### 3 Atomistic simulations

Understanding of the diffraction pattern evolution presented in the next section can be learned from theoretical simulations. We simulate various stages of surface segregation using atomistic models of PdAg alloy in form of crystallites

having shape of cubooctahedron constructed by adding consecutive closed shells of atoms starting from central fcc atom surrounded by its 12 neighbors. This procedure leads to so called magic number cubooctahedra of 13, 55, 147, 309, 561, 923 atoms etc. Our exemplary models consist of 3871 atoms: 1161 Ag and 2710 Pd atoms (resulting in Ag concentration of 0.3). We consider several atomic arrangements, (1) core-shell with Pd atoms at the core, (2) Ag atoms at the core as well as (3) Pd atoms at the core and forming monolayer at the surface. The latter model attempts to mimic situation when Pd atoms are captured at the surface by strong CO chemisorption forces. The modeling involves realistic interactions between atoms. We assume Sutton-Chen  $n$ -body interaction potentials proved to correctly simulate surface relaxation of Pd and performing well for a range of metal elements<sup>12</sup>. For Pd-Ag interaction potential parameters we do not follow mixing rules but derive parameters on the basis of experimental value of enthalpy of alloy creation<sup>13</sup>. The parameters used were:  $a(\text{PdAg})=3.9887\text{\AA}$ ,  $c(\text{PdAg})=72.5438$ ,  $n=11$ ,  $m=7$ ,  $\text{eps}(\text{PdAg})=0.005801$ . All the listed above models were energy relaxed and from each minimum energy model the powder diffraction pattern was calculated following Debye summation formula. Two other models were calculated starting from the first and the third of the above mentioned. The first (4) probes free energy configurational minimum of the cluster following Metropolis algorithm in Monte Carlo scheme<sup>14</sup>. The procedure was modified allowing relaxing the structure down to 0.3 eV/Å of maximum allowed potential gradient after every exchange of unlike atoms, before its acceptance/rejection. The last model (5) based on the third, assumes Pd monolayer captured at the surface and these atoms are constrained to stay there during the Monte-Carlo run.

The calculated powder diffraction patterns are shown in fig.3 in a narrow angular range around the 111 reflection to show small changes in their position. Pattern simulations of the alloy following Debye summation formula show changes in the peak position and intensity depending on degree of segregation and concentration profile of the elements within the alloy cluster. The general rule that can be learned from them is that the alloy peak position is closer to that corresponding to the element remaining in the cluster center. Thus cluster alloy peaks shift to growing angles during Ag segregation and the other way round during Pd segregation. The model peaks on the way from Ag segregation to Pd segregation follow continuous shift to lower angles with the peak height initially decreasing to rise with Pd atoms moving towards the surface.

### 4 Results and Discussion

Fig.4 shows analysis of 3 diffraction peaks of fcc metal phase for patterns collected during long time cyclic exposure to CO and He. The procedure of data analysis was reported pre-

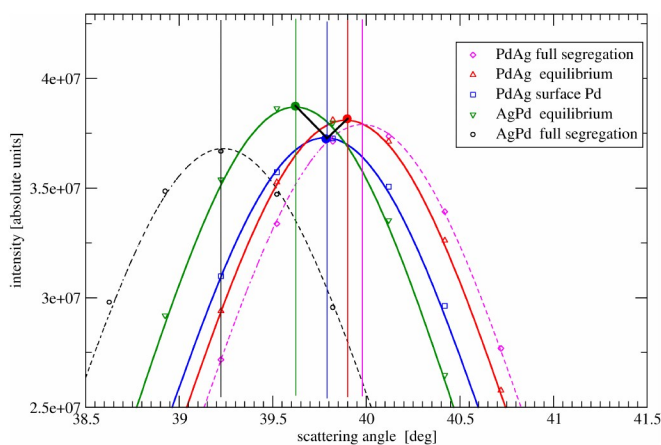


**Fig. 3** Calculated 111 maxima for 5 models of 3871 atom PdAg cluster obtained by energy relaxation (full segregation and core and surface Pd models) and by Monte-Carlo configurational minimization and subsequent energy relaxation (equilibrium models).

viously<sup>10</sup>. The observed structural changes are repeatable - position, intensity and width of diffraction maxima form regular repeatable pattern if one neglect shortening of the CO cycle causing the changes to be not completed. The position and intensities evolution closely resembles the one simulated theoretically (Fig.6) prompting understanding of the experimental phenomena. The experiments clearly show that if the crystallites sintering can be neglected, as in our case, the concentration profile of Ag within the alloy can be to large extent controlled. In CO atmosphere at temperatures above 600K starts slow process of Pd segregation, Pd being kept at the surface by strong chemisorption forces. Such process has been predicted theoretically using DFT methods<sup>16</sup>. It is already established knowledge that Pd chemisorbs strongly CO<sup>17,18</sup> but pure Ag does not. For bimetallic alloy, CO chemisorbs on Pd atoms but not on Ag atoms<sup>19,20</sup>.

We have also considered process of CO disproportionation at the metal surface and a possible saturation of the lattice with carbon that should also effect in lattice constant increase similarly like Pd segregation. This possibility was investigated and plays no important role as proven by the following arguments: (a) We do not observe production of CO<sub>2</sub> higher than in a repeated experiment with no sample. This shows that the recorded during exposure to CO reaction yield is due to the camera steel heating block where the reaction runs. (b) We record repeatable effect with decrease of the lattice constant after heating in He. No traces of methane or other hydrocarbon evolution is detected. The exposure to He may shift the equilibrium but provides no effective mechanism of the surface carbon removal. It is thus unlikely to have carbon dissolved in the alloy or remaining at the alloy surface. (c)

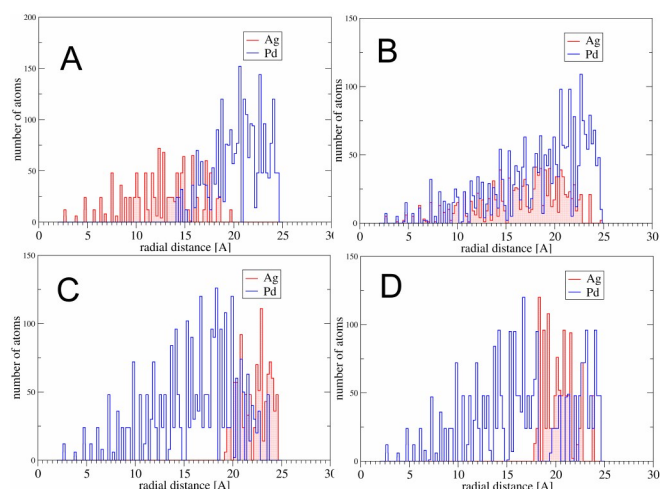


**Fig. 4** Histograms of Pd, Ag atom numbers around the cluster center. (A)-Ag core-Pd shell, (B)-MC optimized (500K) AgPd with Pd constrained to the surface, (C) - Pd core-Ag shell, (D)- Pd core-Ag-Pd surface

To confirm the Pd segregation after heating in CO we have performed catalytic experiments using the sample of PdAg after heating in CO and after heating in He. The reaction monitored structurally and by MS was CO oxidation (PROX) with stoichiometric amounts of CO and O<sub>2</sub> (2:1) (flow rate 20 ml/min and 10 ml/min respectively), at temperatures 498K, 475.5K and 453K. From the MS detected pressures of mass 44 (CO<sub>2</sub>) we have subtracted pressures of mass 44 detected at the same temperatures in a blank experiment, within the XRD camera, with porous glass disc but without the PdAg sample. The stainless steel camera heating block shows considerable activity in PROX and the CO<sub>2</sub> yield in the blank experiment follows closely the yield for the sample heated in He (673K). On the other hand the sample heated in CO (673K) compared to the blank experiment, shows in PROX significantly higher CO<sub>2</sub> yield. The logarithm of difference pressure versus  $(kT)^{-1}$  is nicely linear (considering only 3 points measured) and suggests for this reaction activation energy equal to 0.854 eV (19.7 kcal/mol). This value is slightly lower than reported in literature for Pd (22-33 kcal/mol)<sup>21</sup> what we attribute to the highly strained state of Pd at the surface of crystallites containing Ag having much higher lattice constant (4.08 vs 3.89 Å). Such effect was observed in the literature and predicted theoretically<sup>22-24</sup>. This experiment results are however a convincing proof that after heating in CO, Pd is segregating to the surface, as Ag shows no activity in PROX<sup>19,20,25</sup> similarly as silica support<sup>19</sup>.

Evolution of position and intensity of the measured diffraction peaks at 673K (figs 5,6) shows slow process of Pd segregation in CO (10%CO,90%He) followed by relatively quick segregation of Ag in helium. The evolution is repeatable

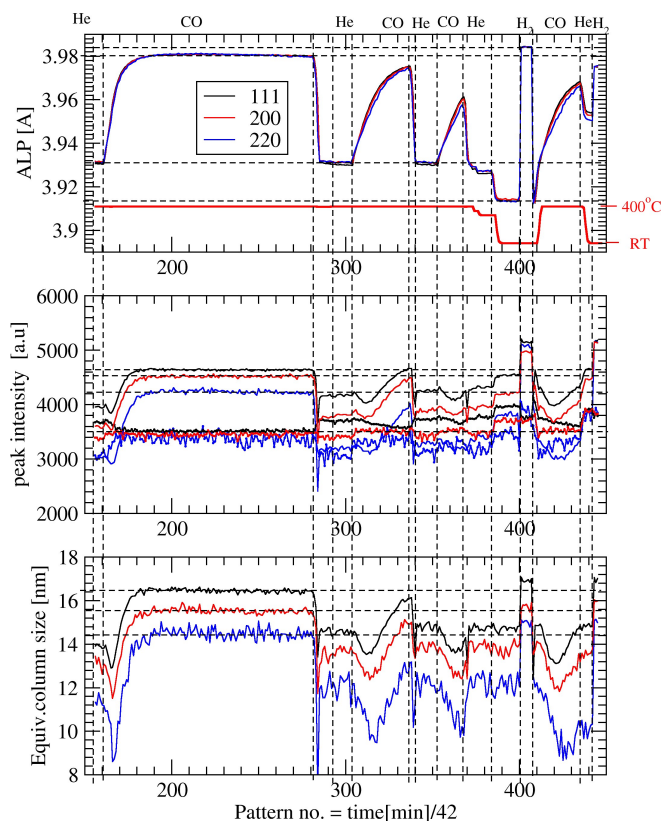


**Fig. 5** Experimental evolution of the alloy 3 peaks apparent lattice parameter (ALP), intensities and equivalent column size in a given crystallographic direction. ALP term is routinely used for nanocrystals where for small sizes various peaks may point to different, not real lattice parameter<sup>15</sup>. The column size derived from Scherrer equation is equivalent in a sense that it corresponds to the peak width taking no account of a possible strain. Indeed the detected column size evolution shows cyclic peak broadening that is evidently due to widening distribution of the lattice parameters during the segregation process. In smaller crystallites the process runs quicker.

besides some initial differences. The process starts from quick decrease of the diffraction peak intensity, followed by continuous rise up to the final state of equilibrium Pd segregation driven by CO chemisorption. The reverse process is nearly two orders of magnitude quicker - in He, Ag segregation at 673K is completed in about 2 hours. During initial phase of the Pd segregation, the equivalent column size displays steep minimum what is evidently an effect of peak broadening due to the observed slow rate of segregation. On smaller particles the process is finished with maximum peak shift when on larger particles it is still at the initial phase. The effect of sample inter-grain diffusion delays or the effect of different time to capture Pd atoms at the surface of different size NPs causing desynchronization of the process, is unlikely

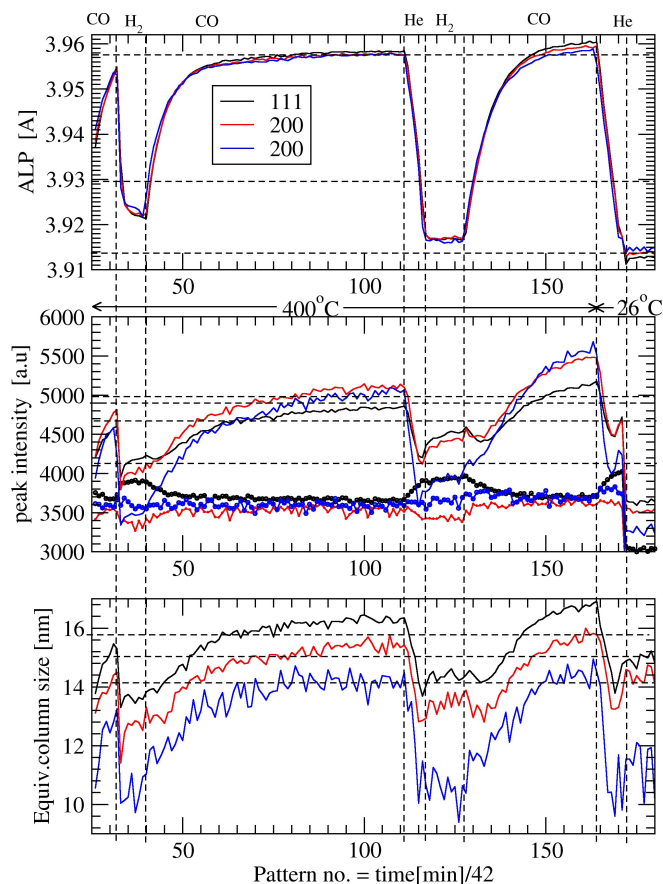


**Fig. 6** Experimental evolution of the alloy 3 peaks apparent lattice parameter (ALP), intensities and equivalent column size in a given crystallographic direction. Measurement started on the other uniformed in CO sample. Note a partial Pd segregation at 673K in hydrogen.

due to a long XRD scan time (42 min per pattern).

Comparison of the experimental observations with models suggests the following atomistic scenario of the process. In He, Ag segregates to the crystallite surface due to lower heat of vaporization. This suggests that the surface is in equilibrium with the neighbor gas phase where Ag vapors have a significant concentration. The Ag surface is quite mobile and surface migration of Ag atoms often causes covering of the surface vacancies initiating lattice vacancy bulk migration that, after some time, ends up again on the surface where the vacancy is filled. The surface serves then as a source and drain for lattice vacancies significantly speeding up the bulk diffusion. On exposure to CO the appearance of CO molecules close to the surface results in occasional capture of Pd atom on its random migration path. This immobilizes the Pd atom at the surface due to high energy of chemisorption. Decreasing the surface

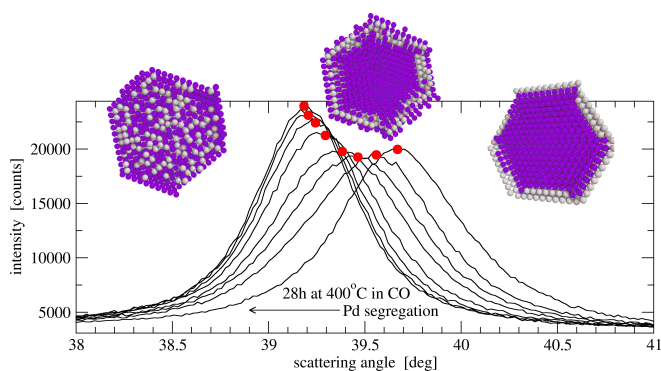


Fig. 7 Evolution of 111 alloy peak during Pd segregation.

still covered by Ag limits its mobility and makes creation of vacancies less likely than their vanishing. This should quickly lead to its depletion down to zero. Thus, after formation of Pd monolayer at the surface the metal self-diffusion is significantly slowed down. It now proceeds following different mechanism as the vacancies are lacking. Whether it is a collective ring mechanism or interstitial remains an open question. This period of slow diffusion is confirmed experimentally leading finally to the equilibrium state in which Ag concentrates in the centers of crystallites.

The experimentally observed by us at 673K in CO atmosphere surface segregation of Pd lasts about 35 hours with its quickest phase of about 12 hours. The Ag segregation in He was recorded as finished after 4 hours. Comparing this phenomenon to a classic Fick diffusion would result in the mean square distance (assumed as a square of half of cluster radius  $r/2$ ) equal to  $Dt$ , where  $D$  is the diffusion coefficient and  $t$  - time. Then, for the Pd segregation the equivalent diffusion coefficient  $D$  would be equal to  $2 \times 10^{-22} m^2/s$  and for Ag segregation  $D = 6 \times 10^{-22} m^2/s$ . These values are much smaller than that estimated from bulk diffusion at higher temperatures. E.g. Moss and Thomas<sup>26</sup> calculated mean free diffusion path at 673K for the PdAg alloy with 20% Ag during 1 hour. Pd atom is predicted to diffuse distance of 1100 nm whereas Ag atom only 15 nm. During 12 hours the expected Pd path is thus above 13000 nm and during 4 hours the expected path of Ag atom is 60 nm. Interestingly, the bulk diffusion phenomena point to the much smaller diffusion of Ag compared to Pd. Our results restricted to atoms mobility within the crystallite show opposite tendency. Ag appears as a more mobile element. Evidently the bulk diffusion involves different mechanism with diffusion along grain boundaries, dislocations and likely impurities playing important role. However diffusion of Ag along grain boundaries appears to be fast<sup>27</sup> and its slower bulk diffusion has to have different explanation. At the single cluster level our proposed atomistic model of kinetics of the process fits well to the experimental data and the measure-

ment method offers a well defined test bed for the models. The diffusion of Pd is hindered by the chemical environment draining the lattice vacancies but diffusion of Ag is still much slower than predicted in the bulk.

The slow process described above can be stopped at any time by cooling down the sample below 570K. It is still a temperature range of many catalytic reactions that can run on the catalyst surface of programmed contents. At the beginning of Pd segregation, the Pd monolayer lays on mostly silver underlayers thus suffer considerable stress due to the lattice misfit. It is expected that such strain can significantly modify its catalytic properties<sup>22-24</sup>. Indeed, we have shown increased Pd activity in PROX reaction and in progress are measurements for a nitric oxide reduction with carbon monoxide.

## 5 Conclusions

Phenomenon of strong adsorption of CO on Pd can be employed to uniform PdAg alloys. If sintering can be avoided, the nanoalloy can be subjected to repeatable processes of Pd and then Ag segregation to the surface. The rate of both diffusion phenomena differs substantially. Atomistic understanding of them suggests for both a quite different mechanism as Pd diffusion to the surface runs in environment depleted of vacancies. This recalls old discussion concerning diffusion basics before discovery of Kirkendall effect. The observed by us diffusion transport is slower than the bulk diffusion reported in literature. Evidently the macroscopic diffusion involves different mechanisms with diffusion along grain boundaries, dislocations and effect of impurities. Study of segregation phenomena in nanocrystals can allow insight into more elementary lattice transport. Switching off dominating vacancy mechanism of diffusion allows to study other subtle transport phenomena in alloys.

## 6 Acknowledgment

The work has been financially supported by Research Grant from the Polish Ministry of Science and Higher Education-decision 753/N-COST/2010/0.

## References

- 1 Smigelskas,A.; Kirkendall,E. *Trans. AAIME* **1947**, 171, 130-142.
- 2 Simmons,R.; Balluffi,R. *Phys. Rev.* **1960**, 117, 52-61.
- 3 Simmons,R.; Balluffi,R. *Phys. Rev.* **1960**, 119, 600-605.
- 4 Simmons,R.; Balluffi,R. *Phys. Rev.* **1960**, 125, 862-872.
- 5 Vasilyev,A.D.; Bekrenev,A.N. *Appl.Surf.Sci.* **2000**, 161, 14-19.
- 6 Vasilev,A.D. *Technical Physics Letters* **2003**, 29(1), 60-61.
- 7 Li,G.Y.; Chan,Y.C. *Mat.Sci.Eng.* **1999**, B57, 116-126.
- 8 Zhang,Q.; Guo,X.; Liang,Z.; Zeng,J.; Yang,J.; Liao,S. *Nano Research* **2013**, 6(7), 571-580.

- 9 Rzeszotarski,P.; Kaszkur,Z. *Phys.Chem.Chem.Phys.* **2009**, 11, 5416-5421.
- 10 Kaszkur,Z.; Mierzwa,B.; Juszczyk,W.; Rzeszotarski,P.; Łomot,D. *RSC Adv.* **2014**, 4, 14758-14765.
- 11 Brodowsky,H.; Poeschel,E. *Z. Phys. Chem. N.F.* **1965**, 44, 143159.
- 12 Sutton,A.P.; Chen,J. *Phil.Mag.Lett.* **1990**, 61, 139-146.
- 13 Hultgren,R.; Desai,P.D.; Hawkins,D.T.; Gleiser,M.; Kelley,K.K., Selected Values of the Thermodynamic Properties of Binary Alloys **1973**, ASM, Metals Park, Ohio.
- 14 Kaszkur,Z. *Phys.Chem.Chem.Phys.* **2004**, 6, 193-199.
- 15 Kaszkur,Z.; Rzeszotarski,P.; Juszczyk,W. *J.Appl.Cryst.* **2014**, 47, 2069-2077.
- 16 Loffreda,D.; Simon,D.; Sautet,P. *J.Chem.Phys.* **1998**, 108, 6447-6457.
- 17 Ponc, V., Bond,G.C. *Catalysis by Metals and Alloys* **1995**, Elsevier, Amsterdam.
- 18 Heinrichs,B., Noville,F., Pirard,J.P. *J. Catal.* **1997**, 170, 366-376.
- 19 Heinrichs,B.; Noville,F.; Schoebrechts,J.P.; Pirard,J.P. *J.Catal.* **2000**, 192, 108-118.
- 20 Sachtler,W.M.H. *Catal.Rev.Sci.Eng.* **1976**, 14, 193-210.
- 21 Berlowitz,P.J.; Peden,C.H.F.; Goodman,D.W. *J.Phys.Chem.* **1988**, 92, 5213-5221.
- 22 Rodriguez,J.A.; Goodman,D.W. *Science* **1992**, 257, 897-903.
- 23 Kampshoff,E.; Hahn,E.; Kern,K. *Phys. Rev.Lett.* **1994**, 73, 704-707.
- 24 Mavrikakis,M.; Hammer,B.; Nørskov,J.K. *Phys.Rev.Lett.* **1998**, 81, 2819-2822.
- 25 Soma-Noto,Y.; Sachtler,W.M.H. *J. Catal.* **1974**, 32, 315-324.
- 26 Moss,R.L.; Thomas,D.H. *Trans. Faraday Soc.* **1964**, 60, 1110-1121.
- 27 Balogh,Z.; Erdelyi,Z.; Beke,D.L.; Portavoce,A.; Girardeaux,C.; Bernardini,J.; Rolland,A. *Appl.Surf.Sci.* **2009**, 255, 4844-4847.